JPRS 81249

12 July 1982

China Report

SCIENCE AND TECHNOLOGY

No. 166

FBIS FOREIGN BROADCAST INFORMATION SERVICE

NOTE

JPRS publications contain information primarily from foreign newspapers, periodicals and books, but also from news agency transmissions and broadcasts. Materials from foreign-language sources are translated; those from English-language sources are transcribed or reprinted, with the original phrasing and other characteristics retained.

Headlines, editorial reports, and material enclosed in brackets [] are supplied by JPRS. Processing indicators such as [Text] or [Excerpt] in the first line of each item, or following the last line of a brief, indicate how the original information was processed. Where no processing indicator is given, the information was summarized or extracted.

Unfamiliar names rendered phonetically or transliterated are enclosed in parentheses. Words or names preceded by a question mark and enclosed in parentheses were not clear in the original but have been supplied as appropriate in context. Other unattributed parenthetical notes within the body of an item originate with the source. Times within items are as given by source.

The contents of this publication in no way represent the policies, views or attitudes of the U.S. Government.

PROCUREMENT OF PUBLICATIONS

JPRS publications may be ordered from the National Technical Information Service, Springfield, Virginia 22161. In ordering, it is recommended that the JPRS number, title, date and author, if applicable, of publication be cited.

Current JPRS publications are announced in Government Reports Announcements issued semi-monthly by the National Technical Information Service, and are listed in the Monthly Catalog of U.S. Government Publications issued by the Superintendent of Documents, U.S. Government Printing Office, Washington, D.C. 20402.

Correspondence pertaining to matters other than procurement may be addressed to Joint Publications Research Service, 1000 North Glebe Road, Arlington, Virginia 22201.

JPRS 81249

12 July 1982

CHINA REPORT

SCIENCE AND TECHNOLOGY

No. 166

CONTENTS

PHYSICAL SCIENCES

Briefs
Observatory Notes Solar Flares 1

APPLIED SCIENCES

Particle Beam Weapon State of the Art Discussed
(Peng Yougui; ZIRAN ZAZHI, Mar 82)..... 2

Success of 'Y-10' Called 'Encouraging Step for Civil Aviation'
(GUOJI HANGKONG, May 82)..... 12

Chinese Human Dimensions and Their Application in the Design of Motor Vehicles (Part I)
(Wang Qiyuan, Qi Huiwen; QICHE JISHU, No 2, 1982)..... 15

Human Fuzzy Control Model in Man-Machine Systems
(Long Shengzhao, et al.; YUHANG XUEBAO, 30 Apr 82)..... 22

Criticial Role of Apogee Engine in Geosynchronous Orbit Explained
(Da Yuan; HANGKONG ZHISHI, Apr 82)..... 29

Briefs
Fujian Computer Parts 33

LIFE SCIENCES

Specialists Attend National Kidney Forum
(XINHUA, 2 Jun 82)..... 34

ABSTRACTS

ELECTRONICS

DIANZI XUEBAO [ACTA ELECTRONICA SINICA], No 3, 1982..... 36

GEOLOGY, GEOGRAPHY

ZHONGSHAN DAXUE XUEBAO--ZIRAN KEXUEBAN [ACTA SCIENTIARUM NATURALIUM UNIVERSITATIS SUNYATSENI], No 2, 1982..... 38

METAL HEAT TREATMENT

JINSHU RECHULI [HEAT TREATMENT OF METALS], No 5, 25 May 82..... 40

NATURAL SCIENCES

XIAMEN DAXUE XUEBAO ZIRAN KEXUE BAN [UNIVERSITATIS AMOIENSIS ACTA SCIENTIARUM NATURALIUM], No 2, 1982..... 41

PHYSICS

JILIN DAXUE ZIRAN KEXUE XUEBAO [ACTA SCIENTIARUM NATURALIUM UNIVERSITATIS JILINENSIS], No 2, 1982..... 43

BRIEFS

OBSERVATORY NOTES SOLAR FLARES--Beijing, June 16 (XINHUA)--Astronomers at the Beijing Observatory under the Chinese Academy of Sciences Monday observed two flares on the eastern and western hemispheres of the sun. The flares occurred at 1420 hours, they said, at almost the same time, reaching their maximum simultaneously. The western flare erupted. X-ray hard radiation interferred with short-wave communications on earth for nearly an hour, they said. [Text] [OW160852 Beijing XINHUA in English 0737 GMT 16 Jun 82]

CSO: 4008/188

PARTICLE BEAM WEAPON STATE OF THE ART DISCUSSED

Shanghai ZIRAN ZAZHI [NATURE JOURNAL] in Chinese Vol 5, No 3, Mar 82 pp 214-17

[Article by Peng Yougui [1256 0645 6311], Wuhan University: "Particle Beam Weapons"]

[Text] In recent years particle beam weapons have attracted the serious attention of military sectors, and of scientists and engineers involved in military affairs in all the countries of the world. In China too, periodicals and magazines have run some articles about particle beam weapons. To give readers some further understanding of them, the present article will provide a technical critique.

So-called particle beam weapons gather charged particles (electrons or protons) that have undergone acceleration by a high energy accelerator, or neutral atoms derived from the neutralization of high energy ions, concentrate them into a beam and shoot them at almost the speed of light at a target (antiship guided missiles, antisatellite spacecraft, intercontinental and submarine-launched guided missiles). They use the accumulated energy and thermal effect of these particles to burn through their housings and set off their warhead detonation systems or damage their internal electric components, destroying or neutralizing the target.

A comparison of particle beam weapons with existing intercept weapons shows the following special characteristics: (1) Rapid intercept time. Particle beams are fired at the target at close to the speed of light, which is almost 200,000 times faster than the speed of conventional weapons. In the case of a 1,000-kilometer intercontinental missile, for example, only a few seconds are required from the time of firing of a particle beam weapon until it hits its target, while missile interception would require several minutes at minimum. (2) Powerful destructive force. Use of focused particle beam directional firing, straightness, and target roles eliminates several intermediate links of conventional weapons, thereby greatly increasing energy utilization efficiency. (3) Operation is flexible and reaction is extremely fast. By changing the field current of the magnetic control mirror, the beam's firing direction can be readily changed. As compared with laser weapons, particle beam weapons are of much greater destructive force. For example, to burn a hole in a 5mm aluminum alloy would require a laser beam impact of 1 million joules of energy per square centimeter, while a particle beam would require only 300,000 joules of energy, a

30-fold difference.[1] Furthermore, particle beams are not as easily stopped by apogee cloud layers as are laser beams; thus they have been termed all-weather weapons. Because they possess these characteristics (particularly speed, the flight time to target being virtually ignorable in calculations), they make an extremely ideal strategic defense weapon. If particle beam weapons were deployed in space and their radiation cone used to attack an adversary, their power would be equivalent to that of a large neutron bomb of equivalent weight. However, particle beam weapons also have their weaknesses. Since they must directly hit their target, accuracy requirements are extremely high. An anti-ballistic missile equipped with a nuclear warhead may err by as much as 1,000 meters, but the position accuracy of a particle beam weapon has to be within 1 meter. Particle beam weapons require extremely accurate position tracking systems and accuracy has to be able to be repeatedly corrected in the process of firing. In addition, particle beam weapons must overcome the effects of the earth's magnetic field on the launching track if it is to be able effectively to intercept the target.

Particle beam weapons may be divided on the basis of the electric charge of the particles into charged particle beam weapons and neutral particle beam weapons. On the basis of the position of the weapons facility, they may be divided into satellite-based, land-based, or ship-based particle beam weapons. On the basis of targets for attack, they may be divided into antisatellite, antiguided-missile, or anticruise missile particle beam weapons.

1. Several Key Technologies

The history of research on particle beam weapons is not a long one, and research is still in the exploratory stage. Figure 1 is a schematic drawing of an an imaginary test facility for the production of proton beam weapons, the principles underlying its functioning being as follows: Within a tightly sealed steel sphere capable of withstanding high pressure and high temperatures, a high energy plasma produced by a thermonuclear explosion is directly converted by a magnetic fluid electric power generator into electrical energy, which then goes through an energy storage converter to form high voltage pulses and produce a beam of high power density relativistic electron beams. Using the automatic resonance acceleration method, 10 kilo-ampere protons are accelerated to almost the speed of light and shot into a drift tube for experimentation to verify transmission properties of the beams in air and the destructive mechanism in relation to the target. A weapons system would include, in addition to the equipment used to produce particle beam acceleration, other components such as target tracking, acquisition, identification, target precision tracking, and guidance, coordination and communications components. The particle beams would be just a means of destroying the target. Their function would be analagous to the interception warhead of an anti-air defense missile system. The key technology for particle beam weapons may be currently generally summarized in the following five categories.

(1) Pulse Power Source

Just how much pulse energy do particle beams require to be able to attain their objective of destroying a target. Generally speaking, quantitative requirements for the pulse electric power source will be determined by the

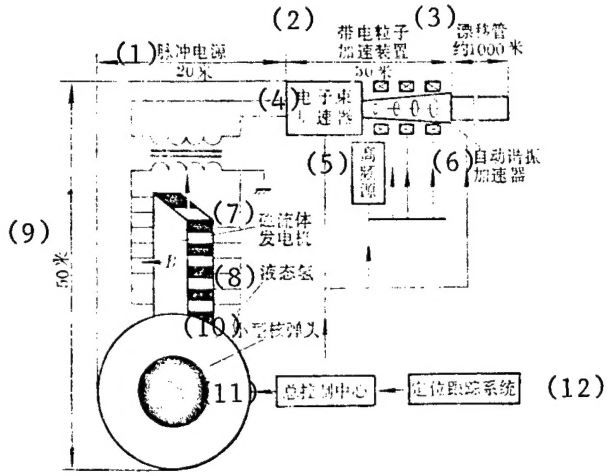

Figure 1

Key:

(1)	Electric pulse source 20 meters	(7)	Magnetic fluid electric power generator
(2)	Charged particle acceleration equipment 30 meters	(8)	Liquid hydrogen
(3)	Drift tube about 1,000 meters	(9)	50 meters
(4)	Electron accelerator	(10)	Small nuclear warhead
(5)	High frequency source	(11)	Main control center
(6)	Automatic resonance accelerator	(12)	Position tracking system

nature of the target to be intercepted by the particle beam weapon, by the distance, transmission situation, and efficiency of the accelerator. Existing data show fairly numerous kinds of destructive effects of particle beams on targets, but mostly they are determined by the energy deposited by the particle beams on the target. (For details, see Table 1). If the pulse energy is 100 megajoules, a neutral beam launched from a satellite can burn a 10^4 square centimeter hole in a guided missile aluminum alloy housing at a distance of 1,000 kilometers. Moreover, a charged particle beam transmitted through the atmosphere requires only 10^5- 10^6 joules of pulse energy to intercept a target 1 kilometer distant.[2] If we use an energy of 1GeV, and a current of 10,000 amperes, electron beams with a pulse width of 1 microsecond can achieve the goal of destroying the aforementioned target. That means the electron beam's pulse power is 10^{13} watts, and the pulse beam's power is 10^7 joules. If the accelerator's efficiency is 30 percent, transmission efficiency not being figured in a pulse power of 3×10^{13} watts would be required. This is an astounding amount, and is 10 times the total sum of all electric power currently generated in the United States.

Just what method may be employed to accumulate such large pulse energy within a single second? Table 2 shows that by using existing electric capacitor or electric inductance methods it is absolutely impossible to satisfy weapons' needs. However, the energy from a thermonuclear explosion (each gram of TNT has a 4,000 joule energy content, and energy released by an atomic bomb is 10^3 as much; energy released from a hydrogen bomb is 10^5 as much) plus its use to drive

Table 1. Minimum Deposited Energy Computation Values for Different Destructive Effects on Several Kinds of Materials

Material	Kind of destruction	Unit energy density ε (Joules/cubic meters)
Aluminum	Melting	3,200
Chemical explosive	Detonation	250
Monocrystalline silicon wafer	Melting	7,000
Monocrystalline silicon wafer	Circuit logic disrupted	1,000
Transistor	Erroneous operation of on-off switch return circuit	25

Table 2. Comparison of Various Kinds of Energy Storage

Type	Energy density (joules/cubic meter)	Attainable energy storage	Release speed (seconds)	Pulse power ratio (watts/cubic meter)
Capacitor	(1/5) 10^2	10^7	10^{-8}	10^{10}
Inductance	(1/4) 10^4	10^8	10^{-1}	(1/4) 10^5
Impulse voltage generator	(1/4) 10^4	10^8	10^{-4}	(1/4) 10^8
Storage battery	(1/5) 10^5	10^8	10^{-3}	(1/5) 10^8
Chemical explosive	10^7	10^8	10^{-7}	10^{14}
Nuclear fission explosion	10^{10}	10^{11}	10^{-7}	10^{17}

magnetic fluid to generate electricity, or else by directly converting it into electric pulse energy for use is the way that offers most hope.

With regard to the magnetic fluid electric power generator, Figure 1 shows it to be different from the ordinary electric power generator. Its conspicuous characteristic is the omission of a prime mover and an improvement in efficiency. Reportedly the pulse fusion used in a magnetic fluid power generator in the USSR produced several hundred million joules of energy from a single reaction.[3] In order to solve problems in storage and conversion, the United States is now actively developing special electric generators that are small in bulk, light

in weight, high in power, and with a high pulse repeating frequency. They hope to be able to supply directly from an electric power generator a high voltage pulse power source to drive a charged particle accelerator.

(2) High Energy Strong Current Charged Particle Accelerator

Particle beam weapons require that the particles fired possess very high speeds, i.e., sufficient power to destroy targets, and the way in which charged particles obtain high energy is the accelerator. The accelerators in operation in the world today may be roughly divided into high voltage low current accelerators and low voltage high current accelerators. Their major parameters are as shown in Table 3. but they are a long way from meeting the requirements of accelerators for particle beam weapons.

Table 3. Characteristics of Two Types of Accelerators and Particle Beam Weapon Accelerator Requirements

Parameters	High voltage, low current accelerator	Low voltage, high current accelerator	Particle beam weapon accelerator
Voltage (mega-electron volts)	1,500	15	1,000
Current (amperes)	0.025	10^5	1,000
Pulse width (nanoseconds)	1.5	0.12	100
Energy per pulse (joules)	56	1.8×10^5	10^8
Pulse repeating frequency	50 cycles per second	several times daily	$\geq$100 cycles/second
Particle beam dispersion (radians)	$\geqslant 10^{-5}$	$\geqslant 10^{-2}$	$\sim 10^{-6}$*

*1 microradian value is all that the weapon system requires outside the atmosphere; when used inside the atmosphere, dispersion will be somewhat more.

A look at available data shows that there are three ways that are most hopeful for developing accelerators to meet weapons requirements as follows: (a) cluster ion accelerators, (b) automatic resonance accelerators, and (c) linear induction accelerators. However, their common characteristic is needed for a strong current relativity electron beam source capable of generating repeated pulses.

For cluster ion accelerators, acceleration of ion clusters is done by shooting strong current pulse relativity electron beams into a drift tube full of thin background gases. The acceleration of a small amount of ions created through ionization of the background gas by the aggregate effect of large numbers of

electrons is very much like a mighty torrent lashing a submerged reef, "small bits of stone" mingling with the turbulent waves after which these "small bits of stone," which are much larger than water molecules, move with the torrent and become accelerated. This is characterized by its not being limited by "electric shock puncture" with the result that the amassed ion acceleration field can reach 10^7- 10^8 volts per centimeter, twice the order of magnitude of the acceleration field of existing accelerators. Now, Luce of the Lawrence Livermore Laboratory (LLL) in the United States uses a powerful pulse electron beam with an energy of 1 MeV, a current of 50 kilo-amperes, and a pulse width of 50 nanoseconds to shoot into an insulated anode vacuum drift chamber with perforations in the middle, thereby obtaining a 1.6 kilo-ampere proton beam at the end of a 50 centimeter long drift tube, the proton energy reaching 45 MeV. Most recent reports tell of using the cluster ion acceleration method to derive ion energy of 200 MeV and a beam strength of 16-20 kilo-amperes, the results of which are rather sizeable.[4]

For the automatic resonance accelerator, automatic resonance acceleration is a combination of the method of accelerating ordinary traveling waves and the cluster acceleration method. This differs from the acceleration of ordinary particle traveling waves as follows. The traveling wave accelerator uses an electromagnetic matrix so that the charged particles being accelerated pick up energy from the traveling wave field and become accelerated. After acceleration, the traveling wave field loses energy, and in order to guarantee continuation of acceleration, it is necessary to continue steady absorption of supplementary energy from outside energy components (such as from high powered beam modulation tubes). The automatic resonance accelerator transmits the powerful current relativistic electron beam inside the drift tube, which has an uneven longitudinal magnetizing field. On the one hand it functions mutually with the traveling waves (i.e., the modulation waves) to make the wave amplitude ever larger, and on the other hand, because of the change in density of the electron beams in transmission, the very strong electric field formed on the surface captures ions from the ionization of the background gases moving them ahead together. The ions thereby absorb energy from the traveling waves and are accelerated to high energy, while the waves also augment their energy from the electron beams. The electron beams are not simply a propagation vehicle for the waves, but also serve as a vehicle for increasing wave strength and field strength and accelerating the ions. Finally comes effectively transferring to the ions the tremendously dense energy stored in the powerful current relativistic electron beams so that the ions will accelerate to high energy.

The automatic resonance accelerator is currently one of the major developmental accelerators in use in the United States. In 1973 Sloan and Drummond of the American Research Association predicted that they could get energy of 0.5 GeV in an accelerating tube no larger than 5 meters long, the beam being a 0.5 kilo-ampere pulse proton beam.[5] Today both the United States and the USSR are actively developing this type accelerator.

The linear induction accelerator. The principle of the linear induction accelerator is to fire powerful current pulse relativistic electron beams into a vacuum drift tube with a series of acceleration gaps, thereby obtaining

acceleration. The Lawrence Livermore Laboratory-designed 50 MeV, 10^4 ampere, 100 nanosecond electron linear induction accelerator is in process of development, and it is anticipated that experiments will shortly begin on long distance transmission directed against various kinds of targets. The repeating frequency used in the experiments will be 5 to 50 times per second, the energy fired at the target each time being 1-10 million joules.[1] Theory estimates that for electron beam weapons with an energy of 500 MeV, a current strength of 10^4 amperes, a pulse width as small as 100 nanoseconds, and six repeating frequencies per second, approximately 20 pulses can hit and destroy a target at more than 1 kilometer.[2] On the basis of current electron beam accelerator technological levels, this figure can be attained with effort.

(3) Beam Transmission

Particle beam transmission is the key to whether particle beam weapons can effectively destroy targets. Because Coulomb repulsion causes charged particles to very quickly disperse or "blow off," when charged particles are transmitted in a vacuum, charged particle beams cannot be transmitted in the near vacuum of outer space. Conversely, because of collisions with air molecules that change the direction of particles when neutral particles are in the atmosphere, they can only be transmitted in outer space or in near vacuum conditions.

The main task of neutral particle beam weapons is to be based on satellites and transmit through outer space to intercept intercontinental guided missiles or space ships at a distance of more than 1,000 kilometers. If at the time they hit the target, the beam's transverse cross-sectional area is 10^4 centimeters^2, the particle beams' divergent angle will have to be less than 10^{-6} radian. Such a requirement is rather high; otherwise the weapon's function cannot be served.

When charged particle beams are transmitted in the atmosphere, the reciprocal function of high energy particles and gas molecules in the air cause energy loss, and also produces an ionization reaction and a Brehmsstrahlung reaction. The ionization reaction makes the surrounding area right next to the transmitted beams form an opposite charge and neutralizes the charged particle beam thereby overcoming the Coulomb repulsion, assuring that the beams will not be scattered in the process of transmission. The Brehmsstrahlung reaction is primarily in the forward direction. Because these two reactions heat up the air surrounding the beams causing a sudden rise in air temperature, when the air pressure drops to 0.1 atmospheres, and the air temperature rises to $\approx$3,000°C, this provides a semivacuum for the next transmission of pulse beams, thereby greatly reducing beam transmission energy loss. This is the so-called "cavity effect," which permits the charged particles to be propagated over a very great distance. It is estimated that for a 1 centimeter^2 cross sectional area in a channel 1 kilometer long a deposit of about 1.5×10^6 joules energy is required. For each kilometer the particle beams travel, the energy loss per electron is 22 MeV. 1GeV energy beams lose only 2 percent of energy. When an electron beam of 1GeV energy and 1,000 amperes is propagated in a channel to a target 1 kilometer distant, the transverse cross sectional area is expanded 4.4 fold thereby assuring use by the electron beam weapon of more concentrated energy to destroy the target. According to data provided by physics constant

tables when particle beams with a power of 1GeV are transmitted through the atmosphere, proton beams can reach 1,420 meters and electron beams 770 meters. If there is repeated pulse frequencing, the propagation distance can be greatly increased.[2]

The aforestated situations are only extrapolations from theory requiring verification. Additionally, problems of channel stability and long distance transmission have to be solved. In addition, the effects of the earth's magnetic field on charged particle transmissions is very great, causing particles being transmitted to deflect. Strength of the earth's magnetic field is a function of position and time, and changes are very great. If precision of the earth's magnetic field is one-thousandth, beam error when transmitted 1 kilometer will be 1 meter. When transmitted 1,000 kilometers, the deviation will be 1 kilometer, making it useless. Therefore, it is presently believed that charged particle beam weapons will find use mostly against targets several kilometers distant. If the laws governing deflection by the earth's magnetic field can be further understood, particle beam weapons can be used with greater precision to destroy targets.

Particle Beams and Target Function Destructive Mechanism

The mechanism whereby particle beam weapons destroy targets is in the nature of three reactions primarily. (a) Causing a hole to be turned in the target housing or burning it to bits. (b) Igniting the warhead, and (c) melting or destroying guidance or control system electronic equipment. For detailed data, see Table 1.

Charged particles possess a powerful penetrating force against light metal housings. A proton with 1 GeV energy can penetrate 60 centimeters thick aluminum, and for each increase in the order of energy magnitude, penetrating ability is increased 40-fold. A 1 GeV electron can penetrate aluminum that is 31 centimeters thick, and for each increase in order of energy magnitude, penetration ability is increased three- to four-fold. Naturally today's missile casings cannot be made 60 centimeters thick, so they are within the range of penetration of high energy particle beams. The Americans, John Parmentola and K. Tsipis believe that if a target at a distance of 1,000 kilometers is to be destroyed (by burning a hole in the missile casing) using a 200 MeV neutral particle beam, a 2×10^{21} particle with a total energy of 6×10^{10} joules would be required.[6] If a pulse beam 100 nanoseconds wide were used, a beam strength of 3×10^{9} amperes would be required, and this is presently unattainable. High energy charged particle beams are also able to cause a series of destructive reactions within the cavity of a missile. Such reactions include neutron reactions, proton reactions, high energy electron reactions, system-generated electro-magnetic pulses (SGEMP), internal electromagnetic pulses (IEMP), or shock waves and thermal waves. Their effect in destruction of the control systems' solid state circuitry would be like "cutting the cranial nerve" of the missile, paralyzing it. In addition, shock waves and thermal waves could directly bring about an explosion, the missile thereby losing its applied force or self-destructing.

(5) Position Tracking System

For particle beam weapons to score direct hits on targets, accuracy requirements are very high. It is generally believed that the high precision aiming and tracking systems used in the development of laser beam weapons can be used with particle beam weapons. The basic methods are to use radar, infrared or optical equipment to measure the target.

Since neutral particle beams do not reflect radio waves, usual radar tracking methods cannot be used; instead a laser resonance scatter method is employed. Low power laser beams excite neutral beams and measurement of the extent of excitation is used to determine the position of the particle beams.

Inasmuch as combat distances are fairly close, in the case of charged particle beam position tracking systems use of a single pulse radar system generally satisfies requirements. At the present time the United States Air Force and the Defense Department Advanced Research Planning Agency (DARPA) are jointly working on development of "space based radar. All-weather searching of large areas will be possible in future, and it will be able to provide data on targets, positions, and speeds. It is anticipated that this radar will go into use during the 1990's. By using a single sensor network, worldwide all-weather detection, tracking, identification and more accurate measurements of targets for particle beam weapons will be possible.

2. Outlook

Judged from the standpoint of physics, partical beam weapons make sense. They possess advantages that existing defensive weapons and laser weapons do not possess. The technical areas on which particle beam weapons touch are very wide, and in terms of current scientific and technical levels, there are no great impediments to their design. However, some problems exist in their deployment. Theoretically transmission distance may be several kilometers, but this has not yet been experimentally verified. Particle beam dispersion, energy attenuation, instability of transmission channels, and the effects of the earth's magnetic field on trajectory when beams are being transmitted are crucial problems for particle beam weapons that await solution. Though stored energy in existing high power pulse technology can attain 5 megajoules, and pulse power can attain 10^{14} watts, neither the speed, volume or on-off repeated frequencies can satisfy particle beam weapon requirements. Additionally, through high energy strong current charged particle accelerators, are designable in principle on the basis of existing technology, and though automatic resonance accelerators and linear induction accelerators are theoretically workable, arduous work will still be required to develop the dimensions and efficiency of accelerating equipment that fully meets weapons requirements. If solutions can be found to the several foregoing problems, the next generation can look forward to particle beam weapons as a strategic defense weapon.

Accompanying the development of particle beam weapons must come the development of nuclear-powered magnetic fluid electric power generation, and research on high energy powerful current charged particle accelerators, and aiming and tracking technology. This must inevitably give impetus to development of nuclear fusion research, laser technology, nuclear fuel production, high speed

movement transient dynamics, nuclear power, and the application to spaceflight technology of nuclear power propulsion. Thus, particle beam weapons research and development plays an important role in advancing modern science and technology.

Enthusiastic help on this article was provided by Comrade Hu Kesong [5170 0344 2646], Zhang Hongjun [1728 4767 6511] and Deng Changdu [6772 7022 1653] of the Ninth Academy of the Second Ministry of Machine Building, for which sincere thanks is given.

REFERENCES

1. Robinson C.A., AVIATION WEEK & SPACE TECHNOLOGY, 110, 14 (1979) 12

2. Robinson C.A., AVIATION WEEK & SPACE TECHNOLOGY, 109, 15 (1978) 42

3. Robinson C.A., AVIATION WEEK & SPACE TECHNOLOGY, 109, 20 (1978) 14

4. He Kesong and Peng Yougui, ZIRAN ZAZHI [NATURE MAGAZINE], 3 (1980) 593

5. Sloan M.L., Drummond W.E., Phys. Rev. Lett., 31, 20 (1973) 1234

6. Parmentola J., Tsipis K., Scientific American, 240, 4 (1979) 38

9432
CSO: 4008/176

SUCCESS OF 'Y-10' CALLED 'ENCOURAGING STEP FOR CIVIL AVIATION'

Beijing GUOJI HANGKONG [INTERNATIONAL AVIATION] in Chinese No 5, May 82, pp 2-3

[Article by staff reporters: "The 'Y-10,' a Chinese-Built Jet Airliner"]

[Text] The Chinese-built jet airliner, "Y-10," was successfully flight-tested in September 1980. Subsequently, additional flight tests were performed, and in December 1981, a transfer flight between Shanghai and Beijing was completed. This achievement was attributed to the persistent efforts of Chinese aeronautical scientists and engineers, government officials, and technicians; it represented an encouraging step forward in China's civil aviation development.

During a tour of the airplane at the airport, we interviewed the design engineers of the "Y-10" to find out the details of the airplane; a summary of this interview is reported below.

The prototype model 01 of the "Y-10" had been used in static destruction tests and no longer exists. It was prototype model 02 that completed the flight between Shanghai and Beijing.

The "Y-10" jet airliner was designed according to international aviation requirements. Its power plant consists of four Pratt and Whitney JT3D-7 turbofan engines suspended from the forward section of the wing. Each engine has a maximum static thrust of 8,615 kg.

Anti-fatigue measures were incorporated in the detailed design of the airplane structure. On parts which are subject to heavy load such as the landing gear, the engine supports, and the flap guiderails, special designs were used to increase the safety margin.

The wing is a single cantilever design with a double-spar, single-plate aluminum alloy structure. The quarter-chord back sweep angle is 33.5°, and the wing profile uses a "spike" airfoil design (early supercritical airfoil) with an upper reverse angle of 7°. It is equipped with leading-edge flaps and double-split trailing-edge flaps. The airplane has good take-off and landing performance and relatively low approach speed. It uses the balancing plate type inner and outer compensation ailerons for lateral control; it is also equipped with inner and outer turbulence guard plates. The use of the "spike" airfoil resulted in a relatively high drag-divergence Mach number (M_d=0.85); its maximum cruising speed can reach 974 km/hr, and its maximum-economy Mach number

for long range flight is around 0.78-0.80. Both the horizontal and vertical tails have a 35° back sweep; the angle of the horizontal tail is adjustable. The elevator and the rudder are both equipped with inner compensation.

The semi-rigid fuselage has an inverted figure "8" cross section and has 87 frames; the sealed cabin extends from frame 1 to frame 74. The passenger cabin is pressurized to 0.6 kg/cm^2. It can accommodate 149 tourist-class seats, 124 mixed-class seats (with 16 first-class seats), or 178 economy-class seats. The cockpit is designed for five crew members (pilot, copilot, engineer, navigator, and radio operator); its windshield meets the field-of-view standards of international civil aviation. Below the fuselage floor there are two luggage compartments whose capacities are 17 m^3 and 21 m^3 respectively.

The landing gears are of the forward three-point design; the forward landing gear has a two-wheel structure which can swivel 56° to the left or right, and can make a 180° turn on a 36-meter-wide runway. The main landing gear is of the four-wheel carriage design.

The control system of the airplane is operated by flexible steel cables. With the exception of the rudder and the turbulence guard plates which are operated hydraulically, all other controls are operated manually by turning the adjustment plate to deflect the control surfaces. All systems are equipped with emergency control devices.

The hydraulic system is operated at a pressure of 210 kg/cm^2; the primary system has two main pumps which are used for operating the landing gears, the flaps, the main brakes, and for controlling the front wheels and the outer turbulence guard plates; the auxiliary system has two electric pumps which are used for controlling the inner turbulence guard plates and the rudder, as well as for emergency situations.

The fuel is stored in the integrated fuel tank inside the wing and the thin-wall soft fuel tank in the mid-wing section. The maximum capacity of the fuel tanks is 51 tons; they can be filled using either a pressurized system or a gravity system. The fuel system is equipped with an emergency dumping device.

The electric system consists of four a.c. generators connected in parallel; each generator has a capacity of 30 kilo-volt-amperes at 120 or 208 volts, and operates at 400 cycles per second. There are also four 75-amp transformer-rectifiers for supplying d.c. electric power. In addition, batteries are available for emergency use.

The electronic equipment include a navigation computer, a weather radar, a doppler radar, a radio compass, a landing computer with omnidirectional indicator and instrumentation, an automatic navigation apparatus, and an atmospheric-data computer. In addition, it is equipped with two shortwave single sideband transmitters, two ultra-shortwave transmitters, an S.O.S. transmitter, and an intercom system.

Key Technical Data

exterior dimensions	
wing span	42.24 m
length	42.93 m
height	13.42 m
wing area	244.6 m^2
interior dimensions	
passenger cabin length	30.4 m
width	3.48 m
height	2.20 m
weight (for domestic flight)	
maximum take-off weight	102 tons
maximum landing weight	86 tons
maximum zero-fuel weight	79.56 tons
maximum payload	21.4 tons
performance	
maximum cruising speed	974 km/hr
economy cruising speed	917 km/hr
maximum climb rate (with maximum take-off weight)	1,200 m/min
maximum cruising altitude	12,330 m
runway length for takeoff	2,070 m
runway length for landing	1,925 m

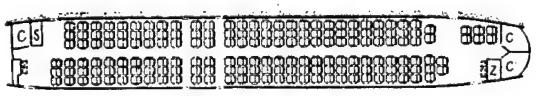

178 seats with 810 mm separation
C. lavatories S. food cabinets
F. seats for stewardesses
Z. storage

Figure 1. Passenger Cabin of the Domestic Model of "Y-10"

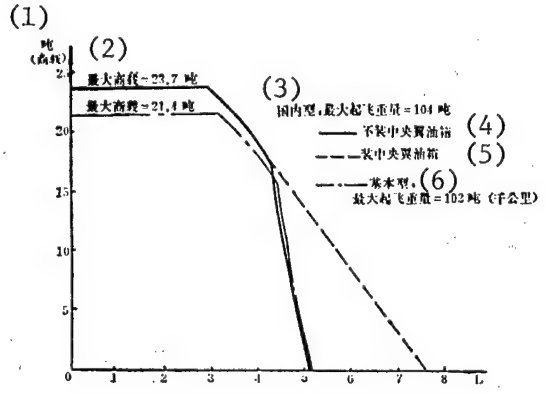

Key:
(1) payload
(2) maximum payload
(3) domestic model, maximum take-off weight=104 tons
(4) without midwing section fuel tank
(5) with midwing section fuel tank
(6) basic model, maximum take-off weight = 102 tons (1,000 km)

Figure 2. Payload-Range Curve of the "Y-10"

3012
CSO: 4008/178

CHINESE HUMAN DIMENSIONS AND THEIR APPLICATION IN THE DESIGN OF MOTOR VEHICLES (PART I)

Changchun QICHE JISHU [AUTOMOBILE TECHNOLOGY] in Chinese No 2, 1982

[Article by Wang Qiyuan [3769 6386 3293], Qi Huiwen [7871 1920 2429]: "The Use of Physical Dimensions of the Chinese People in the Design of Automobiles (Part I)--Brief Introduction to 'The Dimensions of the Driver's Seat of the JB-2667-80 Truck'"]

[Text] I. Physical Dimensions of the Chinese People

In our daily lives and production practices, especially in the building industry, automotive industry, aviation, dressmaking and furniture manufacturing industry that are closely related to people, height and the dimensions of the various parts of the human body are broadly utilized. It is not possible to design the driver's seat of an automobile so that the seat is appropriate, the dimensions are rational, operation is easy and convenient, and the seat is comfortable without grasping the physical dimensions of the human body and the physiological characteristics.

Our nation's regions are vast. There are many people, and the height of the people from various regions varies. How many people should be selected and measured to obtain an "average value" that is believable? Is there any fixed pattern in the distribution of the dimensions of the human body? These should all be solved using the method of "probability and statistics."

1. Sampling of Measurements of the Human Body

We know from previous data that the height of the people in our nation can be classified according to natural regions from north to south into the regions of tall, medium and short people.

The population in the region of tall people constitutes 37.39 percent of the total national population. The population in the region of people of medium height constitutes 30.26 percent and the population in the region of short people constitutes 32.35 percent.

According to date obtained in 1955 from physical examinations of citizens registering for the draft throughout the nation, the standard deviation in the average height σ is 60.1 mm. To improve precision, we take σ = 70 mm. We then take d = 5 mm. According to the formula of the sampling number in probability and statistics.

$n = (\frac{k\sigma}{d})^2$ we obtain:

When the believability of the height for men is 95 percent (K = 1.960), the number of people that we must measure is:

$$n = (\frac{k\sigma}{d})^2 = (\frac{1.960 \times 70}{5})^2 = 753 \text{ (persons)}.$$

When the believability of the height for women is 90 percent (K = 1.645), the number of people that we must measure is:

$$n = (\frac{1.645 \times 70}{5})^2 = 530 \text{ (persons)}.$$

The number of people to be measures and their distribution according to the population ratio of the regions of tall people, people of medium height and short people are shown in Table 1.

Table 1

	Men	Women	Provinces for selected Measurements
Tall people	281	198	Heilongjiang, Jilin, Liaoning
People of medium height	228	160	Zhejiang, Jiangsu, Anhui
Short people	244	172	Sichuan, Yunnan, Guangxi, Guangdong

Then, we measured a number of local people between 18 and 45 years old taking the population of the province as a ratio of the three regions of physical heights. A total of 864 men and 623 women were measured.

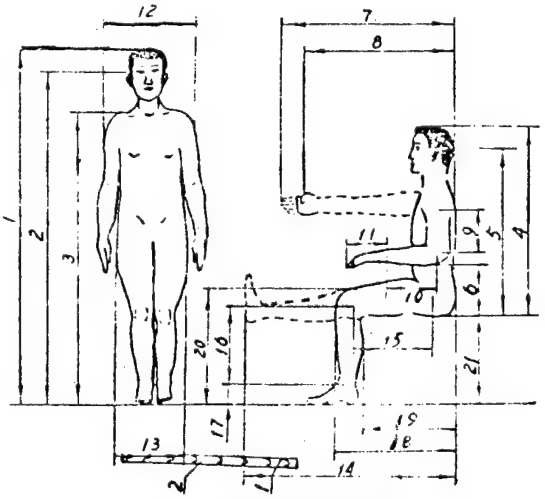

图1 人体尺寸测量项目

Diagram 1

Measurements of the dimensions of the human body

2. Measurments of the human body and results

The parts of the human body selected for measurement are determined according to the needs in driving and in designing the seat. They are mainly the external dimensions and the dimensions of joints of the four limbs.

External dimensions are mainly used to determine the interior space around the driver's seat. The dimensions of the joints of the four limbs are mainly used to determine the range of movement of the four limbs.

There are 21 measurements that have to be concretely determined, see Diagram 1.

The numerical values measured are substituted into the formulas of probability and statistics, and the "average values" and "standard deviations" are computed by computer, as listed in Table 2.

Table 2

(A)序号	(B)测量项目	(C) 男人		(F) 女人	
		均值μ (D)(毫米)	标准差σ (E)(毫米)	均值μ (D)(毫米)	标准差σ (E)(毫米)
1	身长	1688.25	81.83	1586.17	51.29
2	眼高	1585.32	61.61	1480.25	76.02
3	肩高	1420.98	54.35	1320.26	60.96
4	坐高	896.53	36.12	848.52	31.58
5	坐姿眼高	794		743	
6	肘到坐平面	245.23	41.81	238.63	25.63
7	上肢前伸长	837.78	36.81	784.50	37.98
8	拳前伸长	730.87	47.07	688.84	36.79
9	大臂长	269.21	16.36	260.74	19.97
10	小臂长	247.08	13.22	225.93	17.03
11	手长	192.53	9.46	179.00	9.52
12	肩宽	426.32	20.35	391.77	21.67
13	臀宽	333.75	22.62	349.71	23.99
14	下肢前伸长	1015.91	58.91	976.79	50.84
15	大腿长	422.48	28.44	409.21	35.39
16	小腿长	401.34	21.57	368.60	22.21
17	足高	70.69	5.46	65.78	6.94
18	膝臀间距	550.78	27.49	527.77	31.28
19	大腿平长	422.92	23.31	431.76	30.34
20	膝上到足底	515.08	24.67	479.89	23.61
21	膝弯到足底	405.79	19 49	382.77	20.83

Key:

A Number
B Measured part
C Man
D Average value (mm)
E Standard deviation (mm)
F Woman
1 Height
2 Height of eye
3 Height of shoulder
4 Height of hips
5 Height of eye in sitting position
6 Distrance between elbow and hip
7 Length of foward extended upper limb
8 Length of forward extended fist
9 Length of upper arm
10 Length of forearm
11 Length of hand
12 Width of shoulder
13 Width of buttocks
14 Length of forward extended lower limb
15 Length of thigh
16 Length of shank
17 Height of foot
18 Distance between knee and buttocks
19 Average length of thigh
20 Distance between the top of knee and sole of foot
21 Distance from bend of knee to sole of foot

Do the measured results reflect the objective reality of the dimensions of the human body of the Chinese people? Does X represent the centralized tendency of the body of the Chinese people? This problem can be examined on the "normal probability paper."

Taking the height of the male as an example, the measured data can be divided into 22 groups according to height. The number of people in each group, the cumulative number of people, and the cumulative percentages calculated statistically are shown in Table 3.

On the "normal probablity paper" (See Diagram 2), the ordinate represents the statistical percentage of the number of people, and the abscissa represents height. We can see from the diagram that except for the first three points in Diagram 2 which show a slight deviation because of the fluctuation of data, the rest of the points are basically in a straight line. Therefore, it shows that:

(1) the distribution of the dimensions of the human body is a normal distribution;

(2) the sampling number for the measurements is sufficient and the results are correct, reflecting the objective situation of the body of the Chinese people.

Table 3

(1)分组尺寸（毫米）	1600	1610	1620	1630	1640	1650	1660	1670	1680	1690	1700
(2) 人　　数	44	21	29	50	44	44	49	51	45	57	66
(3) 累计人数		65	94	144	188	232	281	332	377	434	500
(4) 累计百分数	5.1	7.5	10.9	16.7	21.8	26.9	32.5	38.4	43.6	50.2	57.9

(1) 分组尺寸（毫米）	1710	1720	1730	1740	1750	1760	1770	1780	1790	1800	以上 (5)
(2) 人　　数	60	58	45	40	45	25	23	23	10	10	25
(3) 累计人数	560	618	663	703	748	773	796	819	829	839	864
(4) 累计百分数	64.8	71.5	76.7	81.4	86.6	89.5	92.1	94.8	96	97.1	100

Key:

1. Group dimensions (mm)
2. Number of people
3. Cumulative number of people
4. Cumulative percentages
5. Over

Diagram 2 Examination of the normal distribution of height of males

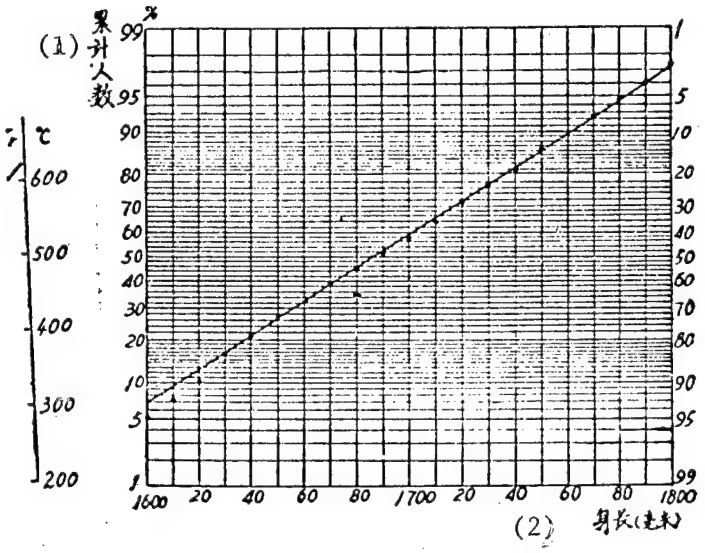

Key:

1. Cumulative number of people
2. Height (mm)

4. Comparison of the physical dimensions of our nation's people and those of foreigners

To make it easy to compare the differences between the physical dimensions of our nation's people and the physical dimensions of the people of other nations so that the characteristics of the physical dimensions of our nation's people and the possibility of foreigners driving the newly designed automobiles can be taken into consideration, we compiled the physical dimensions of Japanese, American, West German and Russian men and listed them in Table 4.

Table 4

(1) 国别 / 数值 (毫米) (2) / 项目 (3)	中国 (16)	日本 (17)	美国 (18)	西德 (19)	苏联 (20)
(4) 身长	1688	1667	1750	1720	1715
(5) 坐高	897	907	913	900	
(6) 坐姿眼高	794		818	790	
(7) 上肢前伸长	838		879	870	
(8) 大臂长	269	284	282		320
(9) 小臂长	247	255	251		275
(10) 手长	193	183			
(11) 肩宽	431		455	450	
(12) 大腿长	422	408	462		410
(13) 小腿长	401	366	414		420
(14) 足高	71	89	83		65
(15) 膝上到足底	515	491	510	550	

Key:

1 Nationality
2 Numerical value (mm)
3 Part
4 Height
5 Height of hip
6 Height of eye in sitting position
7 Length of foward extended upper limb
8 Length of upper arm
9 Length of forearm
10 Length of hand
11 Width of shoulder
12 Length of thigh
13 Length of shank
14 Height of foot
15 Length from top of knee to sole of foot
16 Chinese
17 Japanese
18 American
19 West German
20 Russian

It can be seen from Table 4 that the Japanese are the shortest, Europeans and Americans are the tallest, and the Chinese are slightly shorter than the median height of the two. The "height of the hip" of the peoples of all the nations are about 900 mm, and the differences are not large. Therefore, in setting the interior dimensions of the automobile body, the dimensions "from the surface of the seat to the roof (body and head room)" are not visibly affected. The difference in the height of the people of the various nations is mainly found in the lengths of the lower limbs. Therefore, to enable the driver to operate and control the peddles rationally, the seat of the driver must be appropriately adjustable forward and backward.

(To be continued)

9296
CSO: 4008/146

HUMAN FUZZY CONTROL MODEL IN MAN-MACHINE SYSTEMS

Beijing YUHANG XUEBAO [JOURNAL OF CHINESE SOCIETY OF ASTRONAUTICS] in Chinese No 2, 30 Apr 82 pp 12-17

[Article by Long Shengzhao [7893 0581 3564], Jiang Qiyuan [1203 3217 6678], He Kaiyuan [0149 7030 3293] and Zhao Xu [6392 2485]]

[Text] Abstract: A fuzzy control model for human operators in man-machine systems has been developed using the theory of fuzzy sets to describe the thinking activities in the human mind (concepts, judgment, inferences and decisions, etc.). This model includes seven basic variables, which are: three fuzzy variables (membership function of error judgment, membership function of error rate judgment, membership function of control output), inference rule table, sensor and perception delay, neuromuscular lag and remnant of accidental activity, etc. The agreement between model output and the actual output of human operators has been illustrated by means of an experiment in spacecraft dynamics ($1/S^2$).

Experimental results show that the proposed model can be used to simulate the control action of operators of spacecraft, airplanes, ground vehicles, and ships. The development of this model provides a new approach for studying man-machine systems (e.g., performance prediction, design, and evaluation).

1. Introduction

One of the objects of the study of man-machine systems is the control function performed jointly by man and machine. The joint system is called a man-machine control system or manual control system, in which the human is referred to as the operator. This type of control system has a wide range of applications. In order to apply control theory to analyze this type of system, it is necessary to establish a mathematical model which characterizes the human information input and output relations. This is an important but difficult step in the analysis. Therefore, since the 1940's, the study of mathematical models for human operators has been a topic of great interest [1], and a variety of mathematical models have been developed. Currently, the most commonly used models include: transfer function model [2, 3], optimal control model [4], and time series model [5]. Each of the above models is inadequate in one way or another because human behaviors

have the ability to self-adapt and to learn; and human activities are often non-linear, time-varying, and stochastic. However, the invention and subsequent development of fuzzy mathematics provided a new approach to establish mathematical models of human responses.

It is well known that the distinct feature of a man-machine system is that it contains human elements, which in turn are controlled by thinking activities. The concept of fuzzy sets and the foundation of fuzzy set theory were proposed by Zadeh [6], who modified the theory of ordinary sets by incorporating the features of discrimination and decision-making abilities of human mind about the surroundings. Conversely, to describe human thinking activities using fuzzy set theory is not only necessary but also feasible. In this article, a model is developed to characterize the human thinking activities in a man-machine system, and its effectiveness is illustrated by a practical example.

2. Mathematical Description of the Model

In this development, we consider a man-machine system with a single degree of freedom, and assume that the dynamics of the display and control devices can be neglected. Even if they are not negligible, one can treat them as part of the controlled variables so that the derivation is completely general.

In order for a human to control the machine, he must be able to sense the control error and error rate of the system, and make a judgment based on the sensed information and the preconceived concept stored in the human brain. On the basis of the above judgment, an inference is made to decide what control strategy should be taken. Finally, the required control is produced through neuromuscular response. Because of the stochastic nature of human behavior, a remnant white noise should be superimposed on the final control output. This is the entire process of human control activities, as illustrated in Fig. 1. We assume that the following three domains of investigation are of primary interest:

E--bias error in the controlled parameter from its target value (system input) as sensed by the human operator, simply referred to as error;

R--rate of change of error sensed by the human operator, simply referred to as error rate;

C--control output generated by the human operator, simply referred to as control.

In general, when a human engages in control activities, many concepts in his thinking process are fuzzy. For example, in operating a spacecraft, if the pitch attitude of the spacecraft deviates from its target value, causing it to pitch up (with "large" or "small" error), the astronaut will respond by pushing the control lever forward (with corresponding "large" or "small" control) to return the pitch attitude to its original value. However, the concepts of "large" or "small" errors and controls are all fuzzy in the mind of the astronaut; there is no clear definition of what is meant by "large" or

"small." Nevertheless, through these fuzzy concepts, the astronaut is able to achieve a definite control objective. The situation is analogous in the control of other machines (e.g., airplanes, tanks, ships, etc.). In order to describe these fuzzy concepts, we assume that within each domain of investigation E, R, C, there are seven fuzzy sets: PB, PM, PS, ZE, NB, NM, NS, which represent the concepts of Positive Big, Positive Medium, Positive Small, Zero, Negative Big, Negative Medium, and Negative Small.

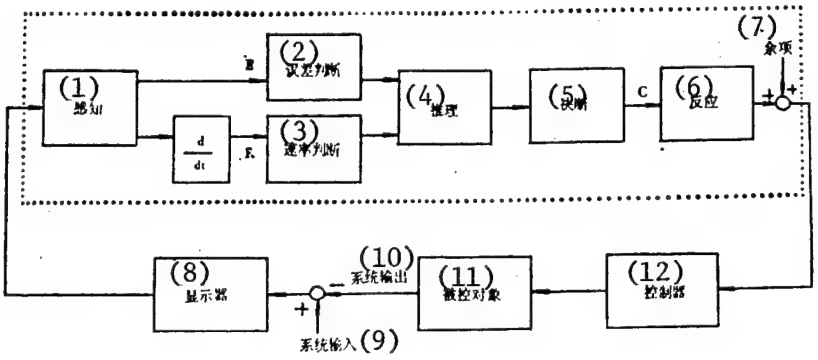

Fig. 1. The Structure of a Human Fuzzy Control Model

Key:

1. Sensation and perception
2. Error judgment
3. Error rate judgment
4. Inference
5. Decision
6. Response
7. Remnant
8. Display unit
9. System input
10. System output
11. Controlled objects
12. Control device

The combination of these fuzzy concepts with a specific domain of investigation forms seven different judgments, or seven different sets, each of which is a fuzzy variable. For example, a judgment "positive big error" is denoted by E_{PB}; the notations E_{PM}, E_{PS}, E_{ZE}, E_{NB}, E_{NM}, E_{NS} have corresponding meanings. Similarly, one can form seven judgments for the error rate: R_{PB}, R_{PM}, R_{PS}, R_{ZE}, R_{NB}, R_{NM}, and R_{NS}. Based on the physiological properties of human beings, it can be stated that human judgments are normally distributed; this fact has been verified by the experimental results of reference [7]. Therefore, both input quantities E and R are normally distributed fuzzy variables. Furthermore, we also assume that human judgments with respect to positive and negative signals are symmetrical. Thus, by using the results of reference [7], the membership function of the above fuzzy variables can be expressed as follows.

For domain E, if $e_1 < e_2 < e_3 < e_4$, then:

$$
\begin{aligned}
E_S(x) &= \begin{cases} 1, & 0 < x \leqslant e_1, \\ e^{-\left(\frac{x-e_1}{\sigma_e}\right)^2}, & x > e_1; \end{cases} \\
E_M(x) &= \begin{cases} e^{-\left(\frac{x-e_2}{\sigma_e}\right)^2}, & 0 < x < e_2, \\ 1, & e_2 \leqslant x \leqslant e_3, \\ e^{-\left(\frac{x-e_3}{\sigma_e}\right)^2}, & x > e_3; \end{cases} \\
E_B(x) &= \begin{cases} e^{-\left(\frac{x-e_4}{\sigma_e}\right)^2}, & 0 < x < e_4, \\ 1, & x \geqslant e_4; \end{cases} \\
E_{ZE}(x) &= \begin{cases} 0, & x \neq 0, \\ 1, & x = 0. \end{cases}
\end{aligned} \tag{1}
$$

For domain R, if $r_1 < r_2 < r_3$, then:

$$
\begin{aligned}
R_S(x) &= \begin{cases} 1, & 0 < x \leqslant r_1, \\ e^{-\left(\frac{x-r_1}{\sigma_r}\right)^2}, & x > r_1; \end{cases} \\
R_M(x) &= e^{-\left(\frac{x-r_2}{\sigma_r}\right)^2}, \quad x > 0; \\
R_B(x) &= \begin{cases} e^{-\left(\frac{x-r_3}{\sigma_r}\right)^2}, & 0 < x < r_3, \\ 1, & x \geqslant r_3; \end{cases} \\
R_{ZE}(x) &= \begin{cases} 0, & x \neq 0, \\ 1, & x = 0. \end{cases}
\end{aligned} \tag{2}
$$

The description of human inference activity is based on the method of reference [8], where the symbols PB, PM, PS, ZE, NS, NM, NB in the domains E, R, C are given the numerical values 3, 2, 1, 0, -1, -2, -3 respectively. During the inference process, the human thinking activity is not reflected as a singular phenomenon. We assume that the range of inference activities of human control can be approximately described by the 49 inference rules shown in Table 1, and can be represented by an expression containing a correction factor α:

$$
C = -\langle \alpha E + (1-\alpha) R \rangle \tag{3}
$$

where α takes on values between 0 and 1; the symbol <n> represents the small integer which has the same sign as n, and whose absolute value is greater than or equal to ($|n| + 0.5$). A wide range of inference rules can be realized by simply adjusting the value of α.

Each rule in Table 1 represents a likelihood inference. For example, the rule represented by the (1,1) element means: "if the error and error rate are both negative big, then the control is positive big." It should be pointed out that the conclusion of the likelihood inference can be called a decision. The phrase in the above sentence "the control is positive big" is a decision. Similarly, the results of reference [7] show that this type

of decision is a normally distributed fuzzy variable and is assumed to be symmetric with respect to positive and negative values, and have seven fuzzy sets. Therefore, for domain C, if $c_1 < c_2 < c_3$, then its fuzzy sets can be expressed as:

$$\begin{aligned} C_S(x) &= e^{-\left(\frac{x-c_1}{\sigma_C}\right)^2}, && x>0; \\ C_M(x) &= e^{-\left(\frac{x-c_2}{\sigma_C}\right)^2}, && x>0; \\ C_B(x) &= e^{-\left(\frac{x-c_3}{\sigma_C}\right)^2}, && x>0; \\ C_{ZE}(x) &= \begin{cases} 0, & x\neq 0, \\ 1, & x=0; \end{cases} \end{aligned} \qquad (4)$$

Table 1. Quantitative Representation of Inference Rule Table (α = 0.3)

		R						
		−3	−2	−1	0	1	2	3
E	−3	3	2	2	1	1	0	−1
	−2	3	2	1	1	0	0	−1
	−1	2	2	1	0	0	−1	−1
	0	2	1	1	0	−1	−1	−2
	1	1	1	0	0	−1	−2	−2
	2	1	0	0	−1	−1	−2	−3
	3	1	0	−1	−1	−2	−2	−3

On the basis of fuzzy set theory, each likelihood inference rule can be described by a fuzzy operation. For example, the rule denoted by the first element can be expressed as:

$$C_1 = E \circ (E_{NB} \times C_{PB}) \cdot R \circ (R_{NB} \times C_{PB}) \qquad (5)$$

The other rules (e.g., C_2, C_3, ...C_{48}, C_{49}) can be expressed in a similar manner. Since the inference process is one of maximum likelihood selection, all the rules in Table 1 can be summarized as follows:

$$\begin{aligned} C = C_1 + \cdots + C_{49} &= E \circ (E_{NB} \times C_{PB}) \cdot R \circ (R_{NB} \times C_{PB}) \\ &+ \cdots + E \circ (E_{PB} \times C_{NB}) \cdot R \circ (R_{PB} \times C_{NB}) \end{aligned} \qquad (6)$$

In equations (5) and (6), the symbols +, ·, x, o denote the fuzzy set operations open, intersection, Descartes product, and combination respectively. In fact, equation (6) summarizes the basic human thinking process (concept, judgment, inference, and decision). A complete fuzzy control model of the human operator can be obtained by adding to this procedure the human sensation-perception delay $e^{-\tau s}$, the neuromuscular lag $1/T_N S + 1$, and the accidental activity remnant r(n) (see Fig. 1). Generally speaking, the

seven parameters of this model are: the three fuzzy variables (E(x), R(x), C(x)), the inference table, the sensation-perception delay τ, the time constant of neuromuscular lag T_N, and the remnant r(n).

3. Model Examples

To illustrate the fuzzy control model for human operators, we present an experimental example of spacecraft dynamics ($1/S^2$). The experiment is as shown in Fig. 2, where the human input (with error E) and output (with control C) are recorded on a magnetic recorder. The data are then processed and reduced on a computer; the error rate R is calculated by taking the first derivative of the error E. The data sampling period is 100 seconds; and the sampling interval is 0.1 second. It should be pointed out that since the human judgment about the error and error rate are always based on data collected over a finite interval rather than the instantaneous values, a smoothing and averaging procedure (with a smoothing length of 5 points) is used in processing the data.

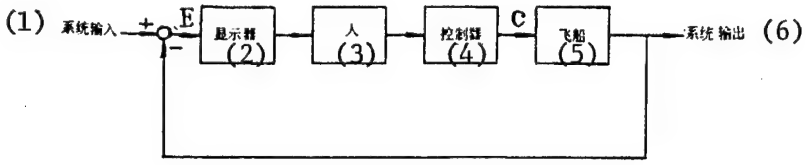

Fig. 2. Block Diagram of a Human-Spacecraft Control System

Key:

1. System input
2. Display unit
3. Human
4. Control device
5. Spacecraft
6. System output

The values of the model parameters are chosen to be: τ = 0.3 sec, T = 0.1 sec, α = 0.3. In order to improve the versatility of the model, a quantization process is applied to the E, R, and C values between zero and 2 standard deviations; also, the range of values of the fuzzy variables E and R are divided into 31 elements:

$$\{E\} = \{R\} = \{x\} = \{-15, -14, \cdots -1, 0, 1, \cdots, 14, 15\};$$

and the values of C are divided into 41 elements:

$$\{C\} = \{x\} = \{-20, -19, \cdots, -1, 0, 1, \cdots, 19, 20\}.$$

Based on the definitions of (1), (2), and (4), we selected the following parameters for the three fuzzy variables: $e_1 = 3$, $e_2 = 7$, $e_3 = 9$, $e_4 = 13$ $\sigma_e = 1.96$; $r_1 = 2$, $r_2 = 7$, $r_3 = 12$, $\sigma_r = 3.10$; $C_1 = 3$, $C_2 = 8$, $C_3 = 14$, $\sigma_C = 2.14$.

Using these parameters, a comparison is made between the model output and the actual operator from experimental data. The good agreement between the

two is illustrated in Fig. 3. It is worth pointing out that these parameters have not been optimized; if parameter identification methods are used to determine the optimum parameter values, the degree of agreement should be further improved. This is a topic for future research, i.e., to solve the problem of parameter identification to improve the effectiveness of the model, and to extract the characteristic parameters of human operators.

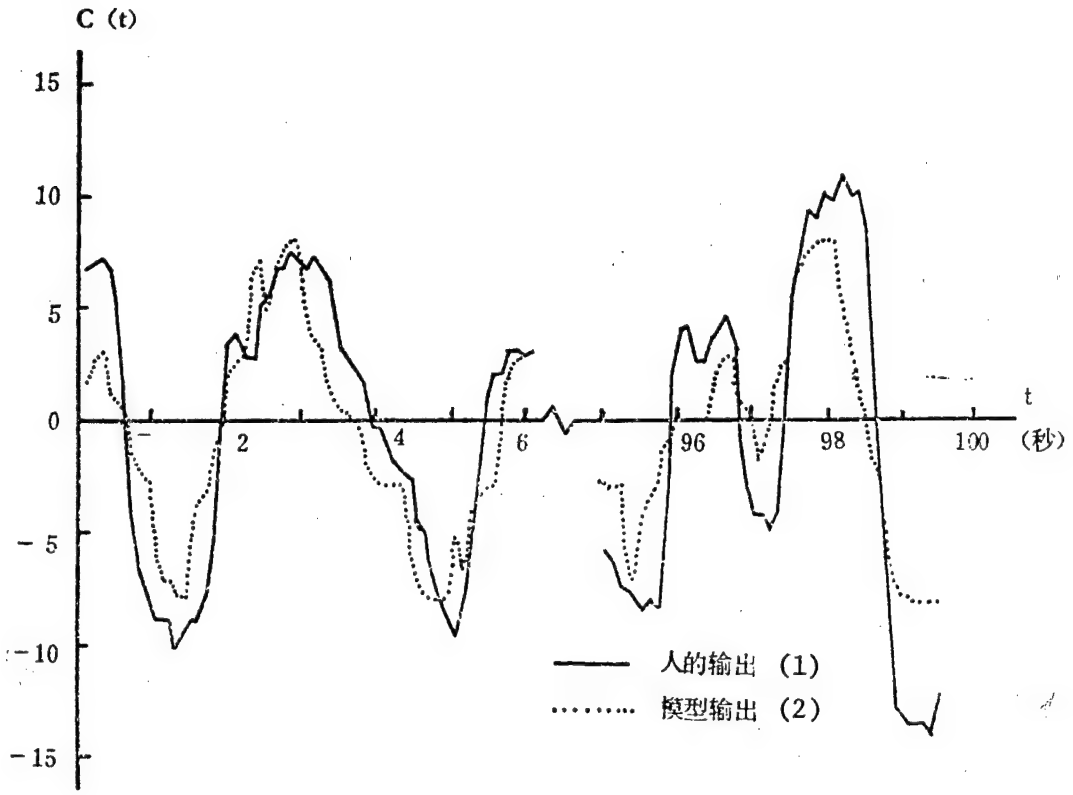

Fig. 3. Comparison Between Model Output and Actual Operator Output

Key:
1. Operator output
2. Model output

4. Conclusion

On the basis of human thinking activities, the theory of fuzzy sets has been used to develop a fuzzy control model for the human operator in a man-machine system. Experimental results show that it is feasible to use a fuzzy control model to simulate human control activities. This model can characterize the behavior of a large class of operators (e.g., operators of space shuttles, space ships, airplanes, automobiles, tanks, ships, etc.). Furthermore, the establishment of this model provides a new approach for studying man-machine systems (e.g., prediction of man-machine system performance, performance design and evaluation, etc.).

3012
CSO: 4008/170

CRITICAL ROLE OF APOGEE ENGINE IN GEOSYNCHRONOUS ORBIT EXPLAINED

Beijing HANGKONG ZHISHI [AEROSPACE KNOWLEDGE MAGAZINE] in Chinese Apr 82 pp 20-21

[Article by Da Yuan [6671 6678]: "The Apogee Engine]

[Text] Modern scientific technology has turned ancient mythology into reality. For example, geosynchronous communications satellites and early warning satellites resemble the mythical "eye that can see a thousand miles" and the "god with all-hearing ears." These satellites provide services in worldwide communications, broadcasting, relaying television transmissions, and in monitoring missile launches thousands of kilometers away. To inject this type of satellite into geosynchronous orbit depends on the apogee engine, which is activated in a transfer orbit several thousand kilometers above the earth's surface.

Orbit Injection

At one of the satellite launch sites, a giant launch vehicle rises from the ground, and one stage after another, it lifts the satellite into a predetermined orbit. Communications satellites and early warning satellites are generally geosynchronous satellites, which are in a circular orbit 36,000 km above the equator, and have a period of 24 hours. In order to make efficient use of the launch vehicle, the satellite is first launched into an elliptical transfer orbit with an apogee of 36,000 km, and having a certain inclination angle with the equatorial plane. The satellite remains in this orbit for several revolutions, during which time it performs the function of orbit and attitude adjustments. Then, when it reaches the apogee, the apogee engine is activated to give the satellite another velocity increment; the final velocity vector, which is in the equatorial plane, places the satellite in a geosynchronous orbit.

The apogee engine is much smaller than the launch vehicle engine, but it plays a critical role in the success of a satellite launch operation.

Engine Structure

The apogee engine is the heaviest component of a satellite, accounting for more than half of the total weight. The INTELSAT 3 weighs 282 kg, of which 160 kg is the apogee engine, including 140 kg of fuel. The apogee engine is

located at the center of the satellite, surrounded by other components (see Fig. 1). Currently most apogee engines used on geosynchronous satellites are solid propellant engines. This type of engine is simple structurally, operationally reliable, and relatively inexpensive. It consists of three parts: the engine housing, the propellant, and the jet nozzle (Fig. 2).

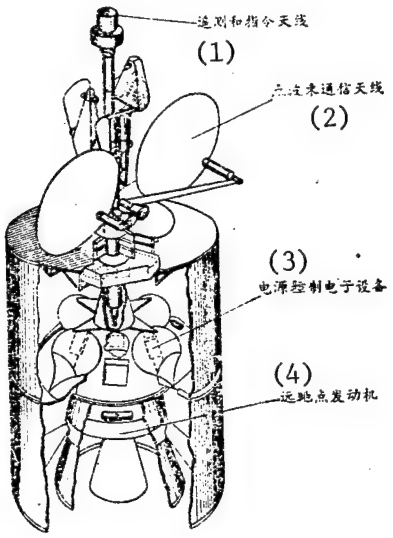

Fig. 1. The Location of Apogee Engine in a Satellite

Key:
(1) telemetry and command antenna
(2) narrow-beam communication antenna
(3) electronic power supply control unit
(4) apogee engine

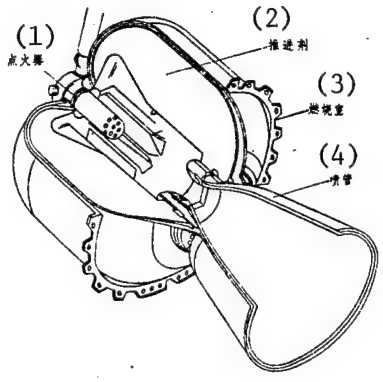

Fig. 2. The Components of an Apogee Engine

Key:
(1) igniter
(2) propellant
(3) combustion chamber
(4) nozzle

The shape of the apogee engine is dictated by the satellite structure. On a spin-stabilized satellite, the apogee engine is shaped like a large top to provide large moment of inertia about the spin axis. Even on a three-axis stabilized (earth fixed) satellite, the apogee engine is limited by the dimensions of the satellite; its shape is quite different from the elongated body of a conventional solid propellant rocket engine.

In the early days, the engine housing was made of steel alloy; later, titanium alloy and fiberglass reinforced plastic materials were used. Fiberglass or organic fiber has smaller specific gravity and high tensile strength; the use of fiberglass significantly reduces the structural weight of the engine. Currently, fiber materials are mostly used on large apogee engines, whereas titanium alloy because of its welding requirement is used on smaller engines.

Apogee engines generally use composite fuels which contain a certain proportion of aluminum powder as combustible. Under the centrifugal force generated by the satellite spin motion, the product of combustion--aluminum trioxide--is deposited in the engine housing. During the combustion process, the deposits can increase the speed of combustion; when the combustion is completed, they tend to raise the temperature of the sidewalls. Generally, the propellant of an apogee engine contains 14 to 15 percent aluminum powder. To further improve the propellant energy efficiency, the current trend is to use high-energy oxident in the propellant.

Apogee engines are generally equipped with nozzles with large expansion ratios. Thrust is generated by expanding the gas through the nozzle. The lower the ambient pressure, the more complete is the expansion, and the higher is the specific thrust (or specific impulse). In this respect the apogee engine is highly efficient because it operates in an environment with practically zero ambient pressure. The expansion ratio (ratio of exit area to throat area) of today's nozzle is approximately 50.

The apogee engine is a high-precision engine; its operational duration and thrust magnitude directly affect the precision of a geosynchronous orbit. Therefore, during the development stage, a series of high altitude simulation tests must be performed; these include simulated tests of high vacuum conditions, complex temperature field conditions, and radiation environment. These tests are necessary to ensure the reliability of engine operation.

Application and Development

Around 1963, the United States launched an experimental geosynchronous satellite called "Syncom." Its apogee engine was made of steel alloy with a mass ratio of only 0.86; the specific impulse (impulse produced per kg of propellant) was only 274 seconds. With the advancement in satellite technology, titanium alloy and fiberglass apogee engines were developed. For example, titanium apogee engines were used on the U.S. "Defense Communications Satellites," the British "Space Net" military communications satellite, the Canadian Communication Technology Satellite "CTS," and the "Geostationary Magnetic Layer Research Satellite" and "Dog Star" satellite developed by the West European nations. For small and medium size satellites, these engines can easily meet the requirements of high performance, high precision, and high degree of reliability.

Later, fiberglass reinforced plastic materials were used in the construction of apogee engines after they had been successfully tested on solid missile engines. For example, the SVM series apogee engines used on the international commercial satellites, the FW-5 apogee engines used on the Canadian domestic communications satellite "Anik," as well as those used on the West European orbit test satellites and maritime satellites "Marots" were all fiberglass solid rocket engines. This type of engine not only has good technical performance but is also relatively inexpensive. Currently, its mass ratio can be as high as 0.9, and its specific impulse is around 290 seconds. The performance of the apogee engine can be further improved by using organic-fiber or carbon-fiber high-energy propellants.

In recent years, a liquid propellant apogee engine was used on the "Symphonie" communications satellite jointly developed by France and West Germany. This engine has a spherical container made of titanium alloy. The container is divided into two compartments for storing two different liquid propellants, which are forced into the combustion chamber using nitrogen gas. The engine has a specific impulse of 311 seconds. This type of engine not only has good performance, but also allows adjustment of the thrust level over a wide range, and has repeated starting capability, so that the satellite has larger flexibility in changing its orbit. This feature has attracted considerable attention in the technical community.

3012
CSO: 4008/173

BRIEFS

FUJIAN COMPUTER PARTS--Fuzhou, 24 May (XINHUA)--Beginning this year, the Fujian electronic computers plant has used domestic parts, increasing by 2.2 million yuan in costs but saving the state 1.05 million dollars in foreign exchange. In addition, it will enable related plants to increase profits by 3 million yuan. A rapidly growing enterprise, the plant has increased its annual output of computers from 5,000 sets in 1979 to 300,000 in 1981, with output value and profits up by 8.3 and 5.9 times respectively. [OW250419 Beijing XINHUA Domestic Service in Chinese 0037 GMT 24 May 82 OW]

CSO: 4008/187

SPECIALISTS ATTEND NATIONAL KIDNEY FORUM

OW021246 Beijing XINHUA in English 1229 GMT 2 Jun 82

[Text] Beijing, June 2 (XINHUA)--Specialists from Beijing, Shanghai, Nanjing and Guangzhou have agreed that the use of a medicinal herb, triterygium wilfordii, in kidney treatment can be measurably effective. About a thousand patients were treated with the herb in various parts of the country.

This was documented in their papers read at a seven-day forum on kidney diseases attended by 150 specialists from across the country, and held by the Chinese Society of Nephrology under the Chinese Medical Association. The meeting closed today.

Specialists said in their papers that they found the therapeutic effect of the herb in the treatment of kidney diseases was somewhat similar to that of steroids, but it is not a steroid and thus possesses no side effects. As a result, it has been welcomed by the steroid-dependent patients.

The herb comes from a kind of deciduous bush with small white flowers and light green leaves, grown in the central and southern parts of China, as well as Taiwan Province. The root can also be prepared as an extract, having an anti-inflammatory effect on bone joints. Doctors in China first used the herb to treat rheumatoid arthritis, then kidney diseases, both to good effect.

During the discussion, a number of the specialists held that the effect of this herb was encouraging and they suggested further study on its therapeutic effect and ways to decrease recurrence should be carried out.

Altogether there were 81 papers read at the forum, covering clinical diagnosis and treatment of glomerular diseases and kidney failure, as well as other experimental studies.

Also attending the meeting were Professor Gabrial Richet of University of Paris, president of the International Society of Nephrology; Professor Priscilla Kincaid-Smith of University of Melbourne, Australia, past president of the society, President Nael S. Bricker of University of California, president of

the 1984 International Congress of Nephrology, and Professor Kenneth Fairley of University of Melbourne. Their papers read at the meeting, dealt with clinical and pathophysiological studies of acute and chronic kidney failure, and were well received.

Experimental and pathophysiological studies on kidney diseases are a new facet of Chinese medical science.

China has used immuno-pathology and electric microscopic examination in diagnosis, kidney transplants and ambulatory dialysis in clinical treatment.

Many hospitals in the country have set up research sections and wards specially for the disease.

CSO: 4008/186

AUTHOR: ZHANG Jialu [1728 1367 7498]

ORG: Institute of Acoustics, Chinese Academy of Sciences, Beijing

TITLE: "Development of Speech Signal Processing and Speech Communication"

SOURCE: Beijing DIANZI XUEBAO [ACTA ELECTRONICA SINICA] in Chinese No 3, 1982 pp 70-78

TEXT OF ENGLISH ABSTRACT: A general outline of the development of speech communication related to the techniques of speech signal processing is given briefly. The development of speech signal processing techniques was divided into three steps: 1) waveform processing; 2) parameter processing; 3) information processing. It is considered that the potentiality of waveform processing of speech is limited, the model of parameter processing of speech has to be developed, and the information processing of speech is still a virgin field.

Some methods of evaluation and diagnosis for speech transmission quality were reviewed and vast vistas of speech communication are anticipated in this paper.

AUTHOR: ZENG Xizhi [2582 6932 0037]
PAN Lihua [3382 0500 5478]
FANG Mingde [2455 2494 1795]

ORG: All of the Wuhan Institute of Physics, Chinese Academy of Sciences

TITLE: "Frequency Synthesizer for Hydrogen Atom Frequency Standard"

SOURCE: Beijing DIANZI XUEBAO [ACTA ELECTRONICA SINICA] in Chinese No 3, 1982 pp 86-89

TEXT OF ENGLISH ABSTRACT: A frequency synthesizer for hydrogen atom frequency standard which has variable six digits has been developed. The frequency of this synthesizer can be changed from 405700.0000 Hz to 405799.9999 Hz with a minimum step frequency of 1×10^{-4} Hz. The measured results show that nonharmonic interrelated spurious output of the synthesizer is less than -85 dB. The measured short term frequency stabilities $\sigma(\tau)$ are 2.07×10^{-11}, 2.48×10^{-12} and 2.88×10^{-13} for averaging time of 0.1s, 1s and 10s respectively. The phase drift of the synthesizer, $\Delta\phi$, is 28.8° when the ambient temperature varies from 20°C to 40°C. No change in output phase of the synthesizer was observed when the supply-voltage varied either from +16V to +19V or from +5V to +6V. The experiments show that it can operate continuously for more than 1 month without trouble, and can operate normally for ambient temperatures from 0°C to 55°C.

AUTHOR: LIU Jiaxing [0491 0857 5281]

ORG: Southwest China Research Institute of Electronics

TITLE: "A Detector-Amplifier with a Wide Dynamic Range and High Sensitivity"

SOURCE: Beijing DIANZI XUEBAO [ACTA ELECTRONICA SINICA] in Chinese No 3, o982 pp 93-96, 30

TEXT OF ENGLISH ABSTRACT: This paper presents a detector-amplifier with a wide dynamic range (about 80 dB) and high sensitivity, and discusses its characteristics of low-noise detection and amplification. The E_n-I_n noise model is analyzed, and based on this analysis the low-noise design principles are developed and three low-noise properties of the detector-amplifier are discussed. Expressions for the detecting sensitivity, dynamic range, etc., are derived by use of the modified Bessel function and the expansion of its series. Some examples of its practical application are also given.

9717
CSO: 4009/331

AUTHOR: HUANG Yukun [7806 3768 1507]
XIA Fa [1115 3127]

ORG: Both of the Department of Geology

TITLE: "The Relation Between Deep Part Structure and Seismicity of the Fault-block Region Along the Northern Coast of the South China Sea"

SOURCE: Guangzhou ZHONGSHAN DAXUE XUEBAO--ZIRAN KEXUEBAN [ACTA SCIENTIARUM NATURALIUM UNIVERSITATIS SUNYATSENI] in Chinese No 2, 1982 pp 17-25

TEXT OF ENGLISH ABSTRACT: The crustal structure characteristics of this region are: one is fault-block, the other is stratified. The seismicity in this region shows that the block-fault displacement is along the horizontal direction and that the interformational sliding is perpendicular to different layers along the fault-block. The latter principally controls the earthquakes of $M \geq 4$.

The seismic focus is distributed along the depth of 5-20 km, which is governed by different seismic layers, one of which is a Conrad surface (about 17-20 km), and the other is the lower discontinuity surface (5-8 km) of the sedimentary overlying strata.

The relative analysis is shown as follows:

[Continuation of ZHONGSHAN DAXUE XUEBAO--ZIRAN KEXUEBAN No 2, 1982 pp 17-25]

1. The earthquakes of $M \geq 4$ are essentially in the plunging edges of the folding uplift and depressive upwarped edges, which are distributed in a narrow banded zone like a sine curve along the Conrad surface.
2. The intense earthquakes are concentrated near the fold hinge point and the axial lines.
3. The characteristics of the migration of deep intense earthquakes and their space and time are rapidly advanced along adjacent symmetrical structure parts of the fold along the Conrad surface. The earthquake interval is from one to several years.
4. The intensity of seismicity is apparently increased in the coincident portions on which the active faulting zones, the sine curves of the fold hinge point of the Conrad surface and the axial lines are projected on the surface.

AUTHOR: LU Ruxiu [4151 1172 4423]
XIE Jinzhao [5509 6930 2507]

ORG: Both of the Department of Geography

TITLE: "The Research on the Law of the Maximum Rising-stage Due to the Typhoon Surge in the Pearl River Estuary"

SOURCE: Guangzhou ZHONGSHAN DAXUE XUEBAO--ZIRAN KEXUEBAN [ACTA SCIENTIARUM NATURALIUM UNIVERSITATIS SUNYATSENI] in Chinese No 2, 1982 pp 26-29

TEXT OF ENGLISH ABSTRACT: The maximum rising-stage of the Typhoon Surge of different estuarine areas and different coastal regions obeys different evolutionary laws. This paper describes the characteristics of the tidal movement and the specificity of physical geography using the comparison method to analyze the regional distribution of the maximum rising-stage.

9717
CSO: 4009/336

AUTHOR: None

ORG: None

TITLE: "Current Condition of Research and Application of Deformation Heat Treatment in China: Excerpt of First National Conference on Deformation Heat Treatment"

SOURCE: Beijing JINSHU RECHULI [HEAT TREATMENT OF METALS] in Chinese No 5, 25 May 82 pp 9-13

ABSTRACT: Deformation heat treatment is a compound work process to cause form and phase variation simultaneously in the reinforcing procedure. This process of combining pressure processing and heat treatment can cause the material or part to have a complex property beyond the capability of a single reinforcing method. As a report of the First National Conference on Deformation Heat Treatment, without mentioning the date and place of the conference, the paper is divided into the following 3 chapters: (1) The position of deformation heat treatment in materials research and its application in metallurgical and machine industries; (2) The condition of research of the theory and application of deformation heat treatment in China; (3) Direction of research in the future. Regarding the condition of basic theoretical research, aspects of high temperature deformation toughening, room temperature deformation and deformation aging, moderate temperature deformation quenching, low temperature deformation quenching, surface deformation heat treatment, and deformation chemical heat treatment are briefly and separately reported.

6248
CSO: 4009/332

AUTHOR: CHEN Boyun [7115 2672 0061]

ORG: Department of Oceanography

TITLE: "The Species Composition and Distribution of the Planktonic Copepods in the Xisha and Zhongsha Islands, China"

SOURCE: Xiamen XIAMEN DAXUE XUEBAO ZIRAN KEXUE BAN [UNIVERSITATIS AMOIENSIS ACTA SCIENTIARUM NATURALIUM] in Chinese No 2, 1982 pp 209-217

TEXT OF ENGLISH ABSTRACT: The present study is based on material collected from the Xisha and Zhongsha Islands, including their adjacent regions, during the period from 1973 to 1975. A preliminary account was made of the species composition and the distribution of planktonic copepods in the region.

As a result of a preliminary examination of the zooplankton samples, 167 species were identified, of which 19 species are recorded for the first time from the South China Sea. The marked dominance of tropical species is clearly shown in the region studied. Among the dominant tropical species, mention should be made of such species as Undinula darwinii, Eucalanus elongatus, Euchaeta marina, Eucalanus subtenuis, etc.

On the basis of the extent of their distribution, the planktonic copepods found in the Xisha and Zhongsha Islands may be divided into four ecological groups: i.e.,

[Continuation of XIAMEN DAXUE XUEBAO ZIRAN KEXUE BAN No 2, 1982 pp 209-217]

1. eurasalinity and eurythermy group; 2. high temperature and low saline group; 3. high temperature and high saline group; 4. deep-water group.

In addition, some species show marked seasonal variation. For instance, warm-water species, such as Temora turbinata, T. stylifera, T. discaudata, etc., occur in winter and spring months. The occurrence of the above species during this period is ascribed to the influence of the Guangdong and Viet-Nan coastal current. In the summer and autumn months, tropical species become dominant due to the influence of the South Sea warm current.

AUTHOR: LIN Changjian [2651 2490 0256]
ZHUO Xiangdong [0587 0686 2639]
TIAN Zhaowu [3944 2507 2976]

ORG: All of the Department of Chemistry

TITLE: "Scanning Micro-reference Electrode Technique for Measuring the Potential and Current Distribution on Micro Areas of Metal Surface"

SOURCE: Xiamen XIAMEN DAXUE XUEBAO ZIRAN KEXUE BAN [UNIVERSITATIS AMOIENSIS ACTA SCIENTIARUM NATURALIUM] in Chinese No 2, 1982 pp 222-225

TEXT OF ENGLISH ABSTRACT: The potential and current density distribution in micro areas on metal surface is significant for studying localized corrosion. A measurement system, scanning micro-reference electrode technique (SRET), is established. The method of preparing micro-reference electrode, the auto-device for scanning electrode and the electronic circuit for automatic recording potential distribution are described.

The electrochemical behaviors of various types of localized corrosion in electrolytes and the mutual influence among active corrosion sites are investigated by SRET. According to the potential contour measured, the active and inactive sites are studied with scanning electron microscope (SEM). The initiation and propagation of localized corrosion are discussed.

9717
CSO: 4009/334

AUTHOR: ZHU Dinghua [2612 1353 5478]
SHAN Fenglan [0830 7685 5695]

ORG: Both of the Department of Physics

TITLE: "The Effect of Rare Earth Elements on the Structure and Properties of Casting High Speed Steel $W_{18}Cr_4V$"

SOURCE: Changchun JILIN DAXUE ZIRAN KEXUE XUEBAO [ACTA SCIENTIARUM NATURALIUM UNIVERSITATIS JILINENSIS] in Chinese No 2, 1982 pp 64-70

TEXT OF ENGLISH ABSTRACT: If the right amount (0.1 - 0.2 percent) of rare earth elements (RE) is added into casting high speed steel $W_{18}Cr_4V$, some properties of the steel will be notable enhanced, e.g., the structure will be raised, and castability, red hardness and cutability will be improved as well. But if the steel contains RE beyond 0.2 percent, the RE inclusions will grow and the mechanical properties will be worse than those of steel without RE.

Based on the observation of cracks, it is revealed that:
1. During the fracture of casting high speed steel almost all the cracks develop along crystal boundaries and the breaking strength is very low.
2. In the steel with the right amount of RE the number of cracks developing along the boundary decreases and the cracks begin to go through the crystal, thus the breaking strength is apparently enhanced.

[Continuation of JILIN DAXUE ZIRAN KEXUE XUEBAO No 2, 1982 pp 64-70]

3. In the steel with too much RE, the majority of cracks develop through the crystals, and the breaking strength decreases, with many RE inclusions near the cracks.

AUTHOR: JI Tao [4764 3447]
CHENG Guobao [4453 0948 1405]
HAN Xiuwen [7281 4423 2429]

ORG: All of the Dalian Institute of Chemical Physics, Chinese Academy of Sciences

TITLE: "The ^{13}C-NMR Spectra Assignment for Some Alkylpyridines"

SOURCE: Changchun JILIN DAXUE ZIRAN KEXUE XUEBAO [ACTA SCIENTIARUM NATURALIUM UNIVERSITATIS JILINENSIS] in Chinese No 2, 1982 pp 89-96

TEXT OF ENGLISH ABSTRACT: The broad proton decoupled and off-resonance decoupled ^{13}C-NMR spectra of eight alkylpyridines were recorded. All of the resonance lines for these compounds were fully assigned by using J.T. Clerc and Lindeman-Adams' empirical rules of chemical shifts, and the values of some empirical parameters used in the calculation of alkylpyridine chemical shift were recommended. In addition, the influence of chirality on the ^{13}C-NMR spectra was observed in a few of the alkylpyridines.

9717
CSO: 4009/335

END